UC San Diego
UC San Diego Previously Published Works

Title

A Multiple Description Coding and Delivery Scheme for Motion-Compensated Fine Granularity Scalable Video

Permalink

Journal

ISSN

Authors

Chan, Yee Sin
Cosman, P. C.
Milstein, L. B.

Publication Date

DOI

A Multiple Description Coding and Delivery Scheme for Motion-Compensated Fine Granularity Scalable Video

Yee Sin Chan, *Member, IEEE*, Pamela C. Cosman, *Fellow, IEEE*, and Laurence B. Milstein, *Fellow, IEEE*

Abstract—Motion-compensated fine-granularity scalability (MC-FGS) with leaky prediction has been shown to provide an efficient tradeoff between compression gain and error resilience, facilitating the transmission of video over dynamic channel conditions. In this paper, we propose an n-channel symmetric motion-compensated multiple description (MD) coding and transmission scheme for the delivery of scalable video over orthogonal frequency division multiplexed systems, utilizing the concepts of partial and leaky predictions. We investigate the proposed MD coding and transmission scheme using a cross-layer design perspective. In particular, we construct the symmetric motion-compensated MD codes based on the diversity order of the channel, defined as the ratio of the overall bandwidth of the system to the coherence bandwidth of the channel. We show that knowing the diversity order of a physical channel can assist an MC-FGS video coder in selecting the motion-compensation prediction point, as well as on the use of leaky prediction. More importantly, we illustrate how the side information can reduce the drift management problem associated with the construction of symmetric motion-compensated MD codes. We provide results based on both an information-theoretic approach and simulations.

Index Terms—Cross protocol layer designs, diversity, drift management, fine granularity scalability (FGS), leaky prediction, motion-compensation prediction, multiple description (MD) coding, orthogonal frequency division multiplexing (OFDM), scalable coding, wireless video.

I. INTRODUCTION

RECENTLY, the emergence of wireless multimedia, specifically wireless video, has triggered a change in design paradigms and research emphases. In particular, to code for dynamic channel conditions, network-adaptive scalable video coding and cross-layer optimization have been under intense research [1], [2]. This is particularly important in a mobile wireless environment characterized by relatively high bit-error rates and bursty-error patterns due to the combination of terminal mobility and time-correlated multipath fading.

Multiple description (MD) source coding has recently emerged as an attractive framework for robust transmission over wired and/or wireless networks [3]. An MD source coder generates MDs; each one individually describes the source with a certain level of fidelity. The multiple bitstreams are transmitted over the network, and the correctly received descriptions are then individually decoded and synergistically combined to enhance the end-user received quality. Due to the individually decodable nature of the MDs, the loss of some of the descriptions will not jeopardize the decoding of correctly received descriptions, while the fidelity of the received information improves as the number of received descriptions increases. In this paper, we propose an n-channel symmetric motion-compensated MD coding and delivery scheme for the transmission of fine granular scalable (FGS) video over orthogonal frequency division multiplexed (OFDM) systems.

Symmetric n-channel MD coding, characterized by $(n + 1)$-tuples $(R, D_1, D_2, \ldots, D_n)$, where D_i corresponds to the distortion for the reception of i descriptions, is a special case of the MD problem in which the distortion depends solely on the number of descriptions received [4]–[6]. Fig. 1 illustrates a practical realization of symmetric n-channel MD [7]–[9] (without motion-compensation prediction) by applying unequal FEC to different parts of an embedded bitstream. As shown in the figure, the embedded bitstream consists of chunks labeled $1, 2, 3, \ldots, n$. These data chunks of decreasing importance are protected by maximum distance separable (MDS) erasure codes with decreasing strength. The availability of *any* one description allows the source data "1" to be recovered, while the successful delivery of any two descriptions allows "1," "2," and "3" to be reconstructed, and so on. As a result, the fidelity improves monotonically as the number of received descriptions increases. This is generally referred as n-channel symmetric FEC-based multiple description coding (FEC-MD) [8]–[11]. FEC-MD has become a popular method for generating MDs for multimedia communications systems such as the Internet [12] and other networks [13]–[15] because of its flexibility of generating arbitrary numbers of descriptions from an embedded bitstream.

FGS video coding was proposed by the MPEG-4 committee to code for dynamic channel conditions and increasing
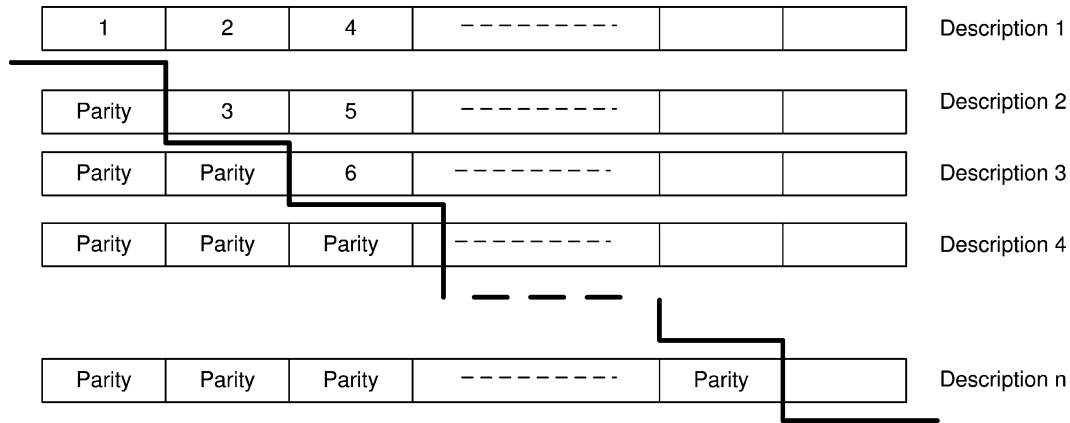
Fig. 1. FEC-MD: n-channel symmetric MD coding using maximum distance separable (MDS) erasure codes.

heterogenous network environments [16]. It partitions the compressed bitstream into a base layer (BL) and a progressively (embedded) encoded enhancement layer (EL) such that the EL can be truncated at any arbitrary location. This specific property addresses the limitation of earlier scalable video coding standards with monolithic ELs [17] (such as H.263+ and MPEG-2) where there is not any partitioning within the EL which may allow less important parts of it to be discarded. As a result, the loss of a portion of the EL may render the entire EL undecodable. This significantly limits the applicability of these codecs in mobile wireless networks.

Most state-of-the-art video codecs incorporate motion-compensated prediction (MCP). With MCP, a single bit error or erasure can cause precipitous degradation due to error propagation as a result of predictor mismatch between the encoder and decoder. This is the so-called "drift" problem. Mismatch between the encoder and decoder can arise from a variety of situations. In motion-compensated MD coding, there are many different predictions that may be used at the decoder, depending on how many descriptions are received [18]. In FGS coding, there exists the potential for different predictions to be used at the decoder, depending on how much of the EL arrives intact.

In the FGS MPEG-4 coder, while the BL is generated by MCP, there is no MCP for the FGS EL. This prediction structure provides an inherent robustness against channel impairments and completely avoids error propagation (drifting effects) due to corruption of the EL. The embedded structure also facilitates the development of prioritized transport protocols and rate control algorithms. For example, one can combine the FGS bitstream with unequal error protection (UEP) using MDS for construction of FEC-MD and achieve a much more robust delivery system [8], [9].

However, due to the lack of MCP in the EL, conventional FGS coding suffers from reduced compression efficiency. To fix this, several algorithms have been proposed in the literature [19]–[21]. The motion-compensated (MC) FGS coding proposed in [19] introduces an MCP loop in the EL (FGS layer) by using the motion vectors (MVs) and prediction modes from the BL. The tradeoff in coding efficiency and error resilience is achieved by controlling the amount of the EL (the number of bitplanes) used for the prediction. However, MC-FGS still suffers from error propagation when the portion of the EL (lower bitplanes) used for prediction is lost. In [20], the authors proposed a progressive FGS (PFGS) coding scheme by adopting a separate MCP loop in the embedded EL. To address the drift problem in the PFGS coding scheme, a prediction path going from the BL to the highest bitplanes of the EL across several frames is maintained so the coding scheme can gracefully recover from channel errors. A robust FGS (RFGS) was proposed in [21] which combines the 2-loop prediction with drift attenuation using leaky prediction techniques. Leaky prediction was first proposed in [22] to improve the performance of a DPCM system in a noisy environment. By scaling down the reference frame by a leak factor $\alpha \in [0, 1]$, error propagation will decay faster in the temporal direction [23]–[25]. The basic idea of these schemes is to partially include MCP in the FGS EL in a well-controlled manner so as to achieve a balance between coding efficiency and error resilience.

In this paper, we first illustrate how the above basic ideas can be extended to the construction of n-channel symmetric motion-compensated MD coding. Based on this, we develop an MD coding-based transmission scheme for the delivery of motion-compensated FGS EL using OFDM systems.

It has been demonstrated that the diversity order of a communication system is an important and integral part for MD transport systems and plays a key role in its robustness [15], [26], [18], [27]. In this paper, we explicitly consider the diversity order of the physical channel and construct an n-channel symmetric motion-compensated MD video coder. Specifically, we demonstrate how knowing the diversity order can assist an FGS predictive coding scheme on the choice of the amount of information to be included in the MCP loop, as well as the choice of the leak factor when using leaky prediction for drift control.

This paper is organized as follows. In Section II, we describe some technical preliminaries, including basics of the channel model used. In Section III, we provide a framework for the construction of n-channel symmetric motion-compensated MD coding. In Section IV, we study the rate-distortion performance of a motion-compensated FGS coder employing both partial and leaky predictions. In Section V, we provide simulation results and discussion. Finally, Section VI gives a summary and conclusions.
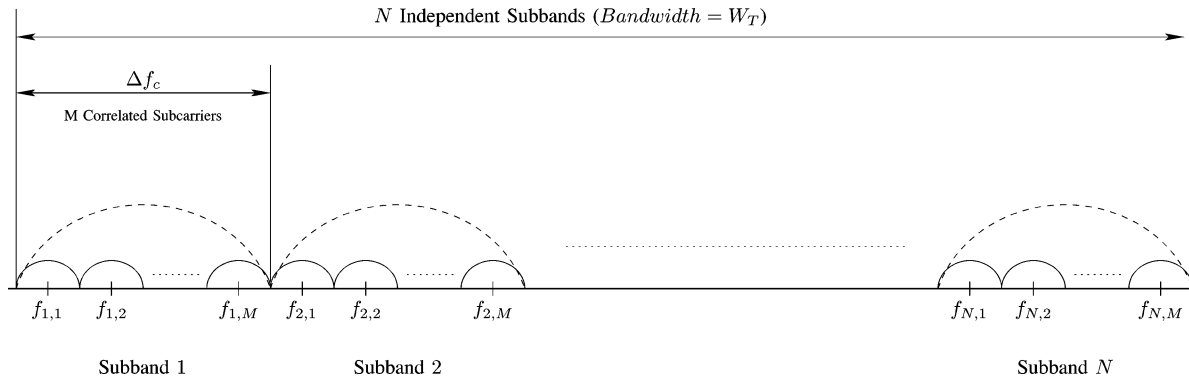
Fig. 2. Subcarrier spectrum assignment.

II. PRELIMINARIES

A. System Description and Channel Model

The basic principle of OFDM is to split a high-rate data stream into a number of lower rate streams that are transmitted over overlapped but orthogonal subcarriers. Since the symbol duration increases for the lower rate parallel subcarriers, the effect of dispersion in time caused by multipath delay spread is decreased. By inserting a guard interval between successive symbols, the problem of intersymbol interference (ISI) is reduced. In practice, this means that symbols are transmitted in parallel over a number of frequency-nonselective (flat-fading) channels.

As illustrated in Fig. 2, we consider a frequency-selective environment and use a block fading channel model to simulate the frequency selectivity. The model has been shown to provide a good approximation to the physical channel, while simultaneously maintaining its analytic tractability [28]–[31]. In this model, the spectrum is divided into subbands whose size equals the coherence bandwidth (Δf_c). Subcarriers in different subbands are considered to fade independently; subcarriers in the same subband experience identical fades.

In particular, let $s[n, m, v]$ be the vth input modulated symbol of a bitstream/description with block length of V modulated symbols at the mth subcarrier of the nth subband. At the receiver end, the output signal $r[n, m, v]$ can be expressed as

$$r[n, m, v] = \alpha[n, m, v]s[n, m, v] + w[n, m, v]$$
$$m \in [1, M], n \in [1, N], v \in [1, V] \tag{1}$$

where $w[n, m, v]$ is a zero-mean complex Gaussian random variable with variance σ^2. We also assume that $w[n, m, v]$ is independent for different n's, m's, and v's. Due to the highly correlated nature of the subcarriers within a subband, we have

$$\alpha[n, m, v] \approx \alpha[n, v] \tag{2}$$

where α is a zero-mean complex valued Gaussian random variable with Rayleigh-distributed envelope.

We assume an OFDM system with an overall system bandwidth W_T, such that we can define N independent subbands. Each of the N independent subbands consists of M correlated subcarriers spanning a total bandwidth of Δf_c. The total number of subcarriers in the OFDM system is equal to NM. In general, the maximum achievable diversity gain is the order of diversity, N. Note that $N = 1$ corresponds to a flat-fading environment, while $N > 1$ corresponds to a frequency-selective environment. In the time domain, we assume the channel experiences slow Rayleigh fading. We do not consider channel coding plus interleaving in the time domain. Generally, due to the bursty nature of the errors associated with a slow-fading environment [32] (as considered in this paper), channel coding plus intrapacket interleaving in the time domain become less effective [33].

B. Overview of Cross-Layer Diversity

To achieve the best performance, MD coding generally requires the existence of *multiple independent* channels [15], [27]. Note that when two individually decodable descriptions are transmitted in highly correlated channels, in most cases, the two descriptions would either be both lost or both received. Hence, relatively little advantage is achieved by using MD coding and making each description individually decodable. However, despite the importance of this fundamental concept, the construction of multiple descriptions is usually considered as a pure source coding technique, in which the existence of multiple independent channels, or, equivalently, the order of diversity, is usually neglected [5], [8], [34]–[37]. The lack of consideration of the order of diversity available may sometimes lead to unnecessarily tight constraints on the construction of MD coders. For example, the construction of a MD coder usually involves having each description *individually* decodable, such that when only one of the descriptions is available, a very low level of fidelity can still be achieved. However, when there are many independent channels, simultaneous failure of all but one of them is unlikely. Hence, the unnecessarily tight constraint that each description be individually decodable leads to inefficient overall system design.

The necessity for considering the diversity order in the construction of MDs has gradually been realized by various researchers, and is applicable in both wired and wireless networks [15], [26], [27]. For example, in [26], multiple independent paths are *explicitly* created at the network layer through routing for the transmission of individually decodable descriptions. This method is sometimes referred to as multiple path transport (MPT), or path diversity.
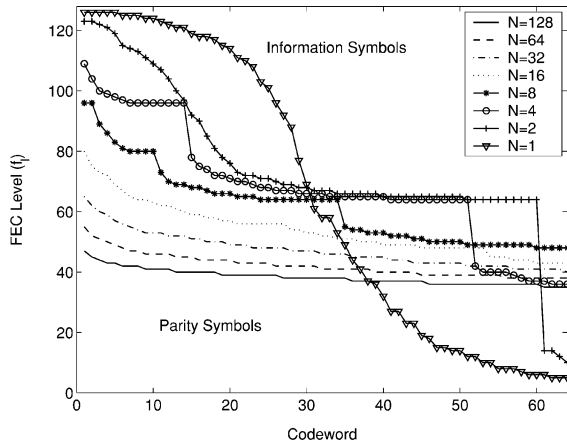
Fig. 3. Construction of cross-layer n-channel symmetric MD codes for an OFDM system with 128 subcarriers, taken from [15]. In the figure, the parameter N denotes the diversity order of the system.

In [15], the authors explicitly consider the number of independent components, or, equivalently, the diversity order, existing at the physical layer in a mobile wireless OFDM system and propose a cross-layer diversity technique which seamlessly combines the concept of channel coding across multiple components and FEC-based MD coding so as to achieve a better system performance. The key results are illustrated in Fig. 3, where the boundaries for the optimal partition of information and parity symbols for n-channel symmetric MD codes are shown for physical channels exhibiting different diversity orders. Each of the curves represents a boundary of the type shown in Fig. 1. The figure clearly indicates the importance of knowing the diversity order for the construction of n-channel symmetric MD codes. In particular, as the order of diversity, N, increases, the degree of tilting of the boundary decreases, indicating less reliance on UEP for optimal performance. The highly correlated nature of subcarriers at low diversity orders also causes stepwise behavior of the boundary due to the high probability of simultaneous loss of the MDs carried by correlated subcarriers.

C. Motion-Compensated FGS With Leaky Prediction

Fig. 4 illustrates the general framework for an MC-FGS coder with leaky prediction [11], [21], [23], [38] which introduces an attenuated MCP into the single FGS EL. In this work, for simplicity, we assume reliable delivery of the BL, including coding modes and motion vectors (MVs) [19], [21]. However, it should be noted that the loss of the BL would cause a substantial degradation of the delivered video quality and sometimes renders the sequence indecodable [11]. Hence, the BL should be well-protected. This can be achieved, for example, by using extensive channel coding.

Since the EL is encoded in an embedded manner, all or part of the EL can be used for prediction for the next EL. The EL MCP loop uses an improved reference frame that combines the BL and the partial EL. As shown in the figure, we denote the partial EL used for MCP as EL-MCP, and the other part used for enhancement only is denoted EL-Extra. If we assume R to be the

bitrate for EL-MCP and $R_{el,\max}$ to be the maximum bitrate for the FGS EL,[1] we can define a parameter $\beta = R/R_{el,\max}$ such that β represents the portion of the EL to be included in the MCP in the EL. As the amount of the EL used for the prediction of the next frame increases, a higher coding efficiency can be achieved. On the other hand, reconstruction errors will accumulate if the portion of the EL used for MCP is not available at the decoder. Hence, β can be used as an adaptive parameter for trading off coding efficiency and error resilience. Note that $\beta = 0.0$ corresponds to the conventional FGS scheme in which the EL is completely excluded from the MCP. As stated previously, FGS can be achieved by employing different coding methods for the residues. Depending on the coding method, β can be defined in different ways. For example, both [11] and [21] considered using the number of bitplanes to trade off the compression efficiency and error resilience. To be independent of the specific encoder implementation, we use the theoretical framework developed by Girod for the study of MCP hybrid coders [39] and allow β to vary continuously. We also verify the results using simulations of real video. More details will be discussed in Section IV where we study the rate-distortion performance of an MC-FGS hybrid coder with leaky prediction.

The leak factor $\alpha \in [0, 1]$ downscales the FGS EL-MCP before it is incorporated into the MCP loop [21], [23], [38]. It is targeted to ameliorate the effects of error propagation caused by the loss of the EL. As a result, the reference $\hat{S}_{el,\beta}^{(n-1)}$ for the prediction of the current EL is a weighted sum of the BL $S_{bl}^{(n-1)}$ and the partial EL $S_{el,\beta}^{(n-1)}$, i.e.,

$$\hat{S}_{el,\beta}^{(n-1)} = (1-\alpha)S_{bl}^{(n-1)} + \alpha S_{el,\beta}^{(n-1)}. \qquad (3)$$

When the leak factor α is set to zero, the EL is also completely excluded from MCP, resulting in the conventional FGS codec, while $\alpha = 1.0$ corresponds to the MC-FGS [11] without leaky prediction which has the best coding efficiency and least error resilience. Hence, by choosing α between 0 and 1, one trades off compression efficiency and error resilience. There are, thus, two separate parameters which we can adjust to trade off between error resilience and compression performance: β, which controls how much of the EL will be used for prediction; and α, which controls how much weight will be given to that EL portion.

In [21], Huang *et al.* showed that the simultaneous utilization of both parameters α and β[2] on a frame-by-frame basis, subject to the bandwidth fluctuation, can greatly improve the delivery of FGS video over wired networks. Similar studies were done by Han and Girod [23], using a multistage embedded quantizer and leaky prediction. In this paper, we will use both parameters for the construction of n-channel symmetric motion-compensated MD coding. A significant contribution of the paper is showing how these two parameters can be optimized explicitly for the order of diversity of an OFDM system.

---

[1]To be consistent with the OFDM system we consider in this paper, we define $R_{el,\max} = 128$ descriptions $\times$ 64 RS symbols/description $\times$ 8 bits/RS symbol $= 65536$ bits throughout the paper.

[2]In [21], β is defined as the number of bitplanes included in the MCP.
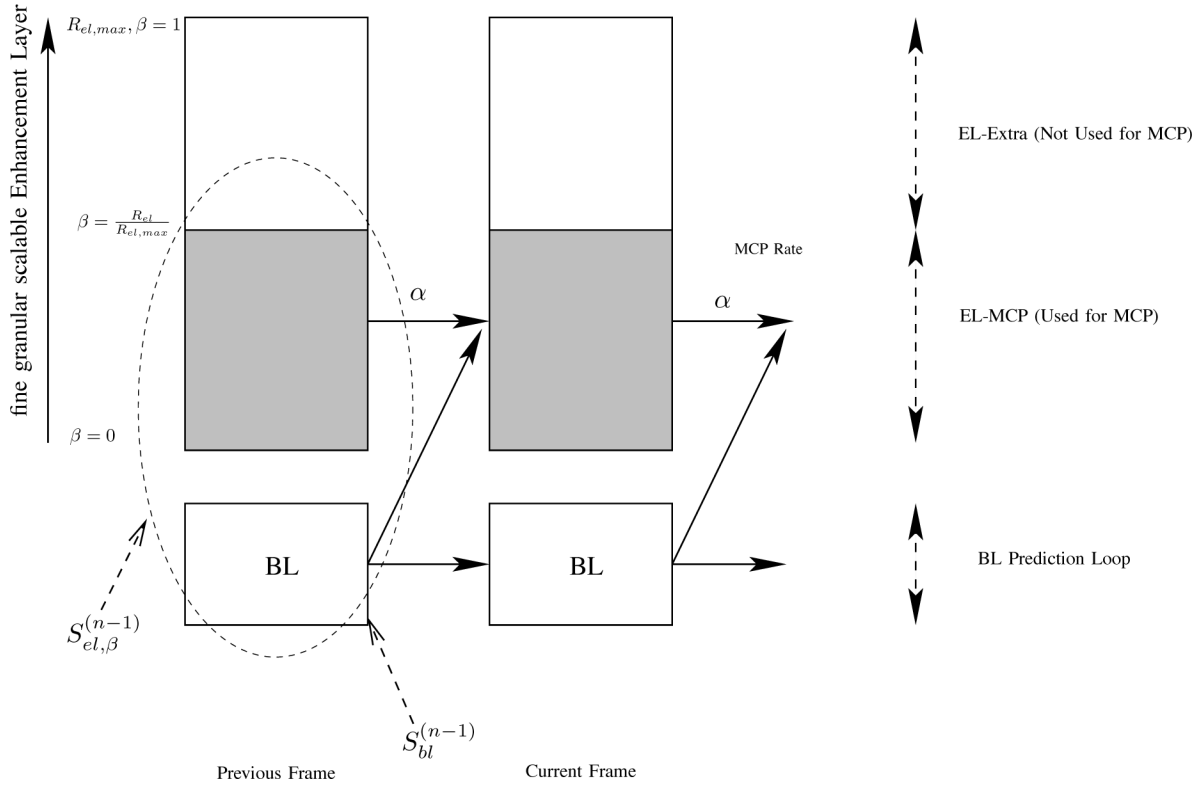
Fig. 4. Motion-compensated FGS hybrid coder with leaky prediction.

III. n-CHANNEL SYMMETRIC MOTION-COMPENSATED MD CODING

A. Drift Management: A Cross-Layer Consideration

Motion-compensated MD video coders face the unique challenge of mismatch control, as a result of the variety of different predictions that may be used at the decoder [18], [40]–[42]. Consider a generic 2-channel nonsymmetric MD system which can be characterized by the quintuple $(R_1, R_2, D_1^{(1)}, D_1^{(2)}, D_2)$, where R_1 and R_2 are the bitrates of the two individual descriptions. $D_1^{(1)}$ is the distortion when description 1 is received, $D_1^{(2)}$ is the distortion when description 2 is received and D_2 is the distortion when both descriptions are received. As a result, there are three possible prediction states at the decoder, corresponding to the successful reception of only description 1, only description 2, or both descriptions (decoded by the central decoder). Each of the three states can form its own prediction loop. Whenever the encoder uses a predictor that depends on a state not available at the decoder, there will be a mismatch between the prediction loops at the encoder and decoder. Similar to single description (SD) MCP coding, this mismatch between encoder and decoder will trigger error propagation, or drift.

To avoid such mismatch, one can, for example, construct two independent prediction loops, each based on a single-channel reconstruction. At the expense of decreased compression efficiency, this can completely avoid the mismatches for the side decoders, even when one of the two descriptions is lost [43], [44]. The method can be extended to $n > 2$ descriptions. For the symmetric counterpart, since the video quality only depends on the number of descriptions received, the two independent prediction loops can be reduced to one. Hence, the symmetric property significantly reduces the complexity of encoding and decoding. In general, there are as many as $(2^n - 1)$ possible prediction states, while there are n prediction states for the corresponding symmetric counterpart. However, when n is large, aside from the complexity issue, the probability of simultaneous failure of all but one of them is typically small. Hence, although this approach completely eliminates mismatches, it is not useful in practice. More importantly, as stated above, "mismatch-free" or "drift-free" approaches generally suffer from poorer compression efficiency [17]. Hence, as opposed to the traditional predictive coding paradigm that systems should not be designed to allow drift/mismatch, there is a growing interest in predictive coding schemes (both SD and MD) that attempt to allow some drift/mismatch so as to improve the overall compression efficiency. This is called the drift-managed approach [23], [40]–[42], [45], [46]. A drift-managed approach does not preclude drift in the prediction strategy. Instead, it allows drift/mismatch to be introduced incrementally, and encompasses drift-free as a special case. In other words, a drift-managed approach optimizes the system performance by trading off the compression efficiency and the amount of mismatch, allowing the drift-free solution to emerge when it is optimal.

The design paradigm can be applied to the construction of n-channel symmetric motion-compensated MD codes. One can, for example, assign $m \in [0, n]$ descriptions as a reference for the temporal prediction, where $m = 0$ corresponds to the drift-free case. Note that if the number of received descriptions $m' <$
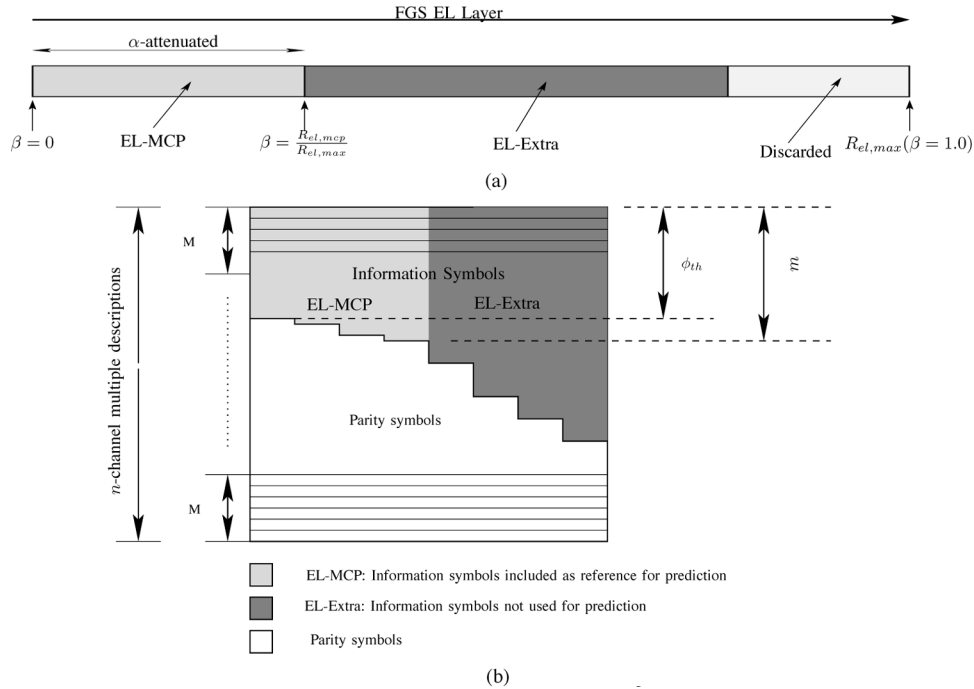
Fig. 5. n-channel symmetric motion-compensated multiple description coding using MDS erasure codes. (a) An FGS (embedded) EL bitstream; (b) motion-compensated FEC-MD coding.

m, there will be a mismatch. Generally, a higher prediction efficiency can be achieved by using a larger m. However, this comes at a price of greater probability of mismatch.

More importantly, although the number of descriptions to be included for the MCP has often been thought of as a "fine-tuning" method for trading off compression and error resilience, and allowing drift to be introduced incrementally (see [18, Section III-G]), the correlation among the subcarriers/channels may make this less effective. For instance, if M out of n descriptions are delivered through M highly correlated channels, i.e., systems with low diversity order, these M descriptions are likely to be lost or received all together. The encoder should decide whether to include M more or M fewer descriptions in the MCP loop, instead of attempting to fine-tune by including one more or one fewer description in the loop, because the correlated nature of the subcarriers makes it unlikely that only one more or one less of description would be received. The effect becomes more significant when M is large, or, equivalently, when the order of diversity is small. This erratic behavior due to the simultaneous loss of several descriptions transmitted through highly correlated channels may greatly affect the degree of encoder-decoder mismatch, and, hence, the effectiveness of drift control, which may subsequently result in severe unexpected error propagation.

B. Motion-Compensated FEC-MD Coding Construction Methodology

In this section, we describe a coding scheme that converts a motion-compensated FGS (embedded) bitstream into n-channel symmetric multiple descriptions using MDS erasure codes. In Fig. 5, we illustrate this construction. In particular, we extend the cross-layer diversity technique proposed in [15], in which multiple independent descriptions are constructed

using an FEC-MD approach, explicitly considering the order of diversity available at the physical layer of a mobile wireless OFDM system. Fig. 5(a) shows a typical FGS EL, in which the bitstream is divided into EL-MCP and EL-Extra. Less important EL-Extra can be discarded as illustrated, based on available bandwidth and channel conditions.

As shown in the figure, similar to the construction of n-channel symmetric MD coding without motion compensation, contiguous information symbols are spread across the MDs. The information symbols are protected against channel errors using systematic (n, k) MDS codes, with the level of protection depending on the relative importance of the information symbols. The reception of at least any ϕ_{th} descriptions out of a total of n descriptions allows us to start reconstructing the source. In the figure, M corresponds to the number of highly correlated subcarriers in a subband, and N corresponds to the number of independent subbands of the frequency spectrum, as shown in Fig. 2. Generally, an (n, k) MDS erasure code can correct up to $(n - k)$ erasures. In Fig. 5, the symbols above the boundary are information symbols, while those below are parity symbols. However, unlike the conventional FEC-MD approach, the information symbols here can be further classified into ones carrying MCP information (i.e., the EL-MCP), and ones carrying information for enhancing the video quality without being used for MCP (i.e., the EL-Extra). EL-MCP is α-attenuated before it is incorporated into the EL MCP loop. Since the number of descriptions used for MCP is m, the reception of $m' < m$ descriptions leads to encoder-decoder mismatch. The extent of the mismatch, and, thus, the degree of error propagation, depends on the difference between m and m' as well as the leak factor α. Intuitively, the amount of mismatch is proportional to $\alpha(\hat{S}_m - \hat{S}_{m'})$, where $\hat{S}_m$ and

$\hat{S}_{m'}$ are the reconstructed frames using m and m' descriptions, respectively.

Mathematically, we formulate the optimization for the construction of n-channel symmetric motion-compensated MDs as follows. Consider a system with N i.i.d. subbands, each with M subcarriers and the packet size of individual descriptions equal to L code symbols. Hence, there are $N_t = NM$ subcarriers (descriptions). We assume that for codeword l, c_l code symbols are assigned to information symbols. The reception of any $m' > \phi_{th}$ descriptions leads to a reconstructed video quality $D(R_{m'})$, where $R_{m'}$ is the information rate, given in terms of the number of MDS symbols

$$R_{m'} = \sum_{\{l : c_l \leq m'\}} c_l. \tag{4}$$

Given the rate-distortion curve $D(\bullet)$ and the packet loss probability mass function $P_{\mathcal{J}}(j)$, where $j = N_t - m'$ is the number of lost packets, which depends on, among other things, the diversity order N of a communication system as well as channel signal-to-noise ratio (SNR), we can then minimize the expected distortion

$$E^*[D] = \min_{\{c_l, \beta, \alpha\}} \left\{ \sum_{j=0}^{N_t - \phi_{th}} P_{\mathcal{J}}(j) D(\beta, \alpha, R_{m'}) + \sum_{j=N_t - \phi_{th}+1}^{N_t} P_{\mathcal{J}}(j) D_B \right\} \tag{5}$$

where D_B corresponds to the distortion when less than ϕ_{th} descriptions are received and so the decoder must reconstruct the video source using the BL only. Note that $R_{m'} < \beta R_{el,\max}$ represents the situation of encoder-decoder predictor mismatch. In this paper, the RD curves $D(\bullet)$ in (5) are obtained using both the information-theoretic approach originally proposed by Girod [39] and real video simulations. Different algorithms can be used to solve the optimization problem [8], [47]–[49] as discussed in [15]. In this paper, we are interested in the construction of FEC-based motion-compensated multiple description coding taking into consideration the order of diversity at the physical layer. Therefore, we use the approach proposed in [8] due to its simplicity. We set the parameter $Q = N_t$ for a full search.

IV. SIMULATION SETUP

The FGS EL is converted to 128 parallel bitstreams using the FEC-based multiple description encoder. The 128 descriptions are mapped to the OFDM system with 128 subcarriers. We use the RS codes for error protection and there are 8 bits per RS symbol. Each description size is set equal to 512 bits, corresponding to 64 RS symbols. Two bytes of cyclic redundancy check (CRC) codes are appended to each description for error detection. Hence, the packet size including the CRC is 66 bytes. We assume slow Rayleigh fading with normalized Doppler spread $f_{nd} = 10^{-3}$ in the time domain. We simulate the channel using the modified Jakes' model [50]. We assume coherent QPSK modulation and set SNR to 20.0 dB. As stated previously, the diversity order of an OFDM system depends on

the ratio of the system bandwidth to the coherence bandwidth. Hence, for a system of 128 subcarriers, the diversity order N can vary from 1 to 128. In this work, we simulate the performance for $N = 1, 2, 4, 8, \ldots, 128$.

A comprehensive information-theoretic rate-distortion (RD) analysis of MCP video coding was first presented in [39]. It relates the power spectral density (PSD) of the prediction errors to the accuracy of motion compensation. The theoretical framework has proved remarkably useful [38], [51], [52], and has provided important guidelines for the practical design of some state-of-the-art video codecs [53]. The approach was used to study single-loop motion-compensated scalable video coding with prediction drift using the optimum forward channel model [54], [55]. It was later extended to the study of the RD performance of a layered video coder with leaky prediction [38].

We assume the PSD of the input video signal to be [39], [51]

$$\Phi_{ss}(\Lambda) = \begin{cases} \frac{2\pi}{\omega_0^2} \left(1 + \frac{\omega_x^2 + \omega_y^2}{\omega_0^2}\right)^{-3/2}, & \text{for } |\omega_x| \leq \pi f_{sx} \\ & \text{and } |\omega_y| \leq \pi f_{sy} \\ 0, & \text{otherwise} \end{cases} \tag{6}$$

where f_{sx} and f_{sy} denote the sampling frequencies when the video signal is spatially sampled at the Nyquist rate. As in [39], we choose $\omega_0 = (\pi f_{sx})/(42.19) = (\pi f_{sy})/(46.15)$, which corresponds to a horizontal and vertical correlation of 0.928 and 0.934, respectively. The parameters are chosen to match the model given by (6) with real video signals [39].[3]

The probability density function of the estimated MV error is modeled as zero mean Gaussian with variance $\sigma_{\Delta d}^2$. Hence, we have the characteristic function given by [39], [51]

$$P(\Lambda) = \exp\left[-\frac{\sigma_{\Delta d}^2}{2} \Lambda \cdot \Lambda\right]$$
$$= \exp\left[-\frac{\sigma_{\Delta d}^2}{2} \left(\omega_x^2 + \omega_y^2\right)\right] \tag{7}$$

and we choose the spatial filter as $F(\Lambda) = P^*(\Lambda)$ as discussed in [39].

Let $R_{E,\text{MCP}}$ be the MCP rate and $D_{E,\text{MCP}}$ be the corresponding distortion. It was shown in [39] and [38] that the RD pairs are

$$R_{E,\text{MCP}}(\theta_{E,\text{MCP}}) = R_B + \frac{1}{8\pi^2} \int \int_{\Lambda} \max\left\{0, \log_2\left(\frac{\Phi_{\psi_E \psi_E}}{\theta_{E,\text{MCP}}}\right)\right\} d\Lambda \tag{8}$$

$$D_{E,\text{MCP}}(\theta_{E,\text{MCP}}) = \frac{1}{4\pi^2} \int \int_{\Lambda} \min\{\theta_{E,\text{MCP}}, \Phi_{\psi_E \psi_E}\} d\Lambda \tag{9}$$

where $\theta_{E,\text{MCP}}$ is the generating parameter, R_B is the BL rate, and $\Phi_{\psi_E \psi_E}$ is the residue PSD of the input signal $\{s\}$ of the BL prediction loop.

---

[3]In [39], the format of the input video signal is 320×288 pixels. Here, to match with the system bandwidth, we consider a QCIF format with resolution 176×144 pixels.

For the information coded above the MCP rate, i.e., the information used for enhancing the video quality but not used for predicting the next frame, the RD performance (R_X, D_X) above the MCP rate can easily be obtained based on Berger's result [54]

$$
\begin{aligned}
R_X(\theta_X) &= R_{E,\text{MCP}} \\
&+ \frac{1}{8\pi^2} \int\int_\Lambda \max\left\{0, \log_2\left(\frac{\Phi_{\tilde\psi_E \tilde\psi_E}}{\theta_X}\right)\right\} d\Lambda \quad (10) \\
D_X(\theta_X) &= \frac{1}{4\pi^2} \int\int_\Lambda \min\left\{\theta_X, \Phi_{\tilde\psi_E \tilde\psi_E}\right\} d\Lambda \quad (11)
\end{aligned}
$$

where θ_X is the generating parameter. $\Phi_{\tilde\psi_E \tilde\psi_E}$ is the residue PSD of the EL prediction loop.

If part of the information used for MCP at the encoder is not available at the decoder, there would be a mismatch in the encoder-decoder MCP loops, which causes drift. The RD pairs (R_M, D_M) due to the encoder-decoder mismatch was derived in [38] to be

$$
\begin{aligned}
D_M(\theta_{E,\text{MCP}}, \theta'_E) &= D_{E,\text{MCP}} + \frac{1}{4\pi^2} \\
&\times \int\int_\Lambda \frac{1}{1 - \alpha^2 |F(\Lambda)|^2} \Phi_{\check\psi_E \check\psi_E} d\Lambda \quad (12) \\
R_M(\theta'_E) &= R_B \\
&+ \frac{1}{8\pi^2} \int\int_\Lambda \max\left\{0, \log_2\left(\frac{\Phi_{\psi_E \psi_E}}{\theta'_E}\right)\right\} d\Lambda. \quad (13)
\end{aligned}
$$

where θ'_E is the generating parameter and $\Phi_{\check\psi_E \check\psi_E}$ is the mismatched PSD.

For real video sequences, the operational RD curves $D(\bullet)$ are obtained based on the H.26L-FGS video codec, comprised of an H.264 TML 9 base layer codec and an EL codec with MPEG-4 FGS syntax. The FGS property is achieved by bit-plane coding. We incorporate both partial and leaky predictions into the codec with a coding scheme shown in Fig. 4. In the simulations, we apply a uniform quantization parameter (QP) value to all blocks of the BL for both I-frames and P-frames. To facilitate the studies, we set BL $QP = 31$ (the largest quantization step) so as to increase the dynamic range of the EL bitrate. The MV resolution in H.264 is set to be $1/4$. The loop filter option is also used. Each sequence is encoded with a frame rate of 30 fps.

V. RESULTS AND DISCUSSION

In this section, we present the results for the construction of the proposed cross-layer coding and delivery scheme using both the information-theoretic approach and simulations of real video. The embedded (FGS) bitstream was converted to 128 parallel bitstreams using an n-channel symmetric motion-compensated FEC-MD encoder incorporating the information on the diversity order of the physical communications system.

A. Partial Prediction: EL-MCP (β)

In Fig. 6, we show the rate-distortion functions of an MC-FGS hybrid coder assuming a source model given by (6) for $\sigma^2_{\Delta d} =$

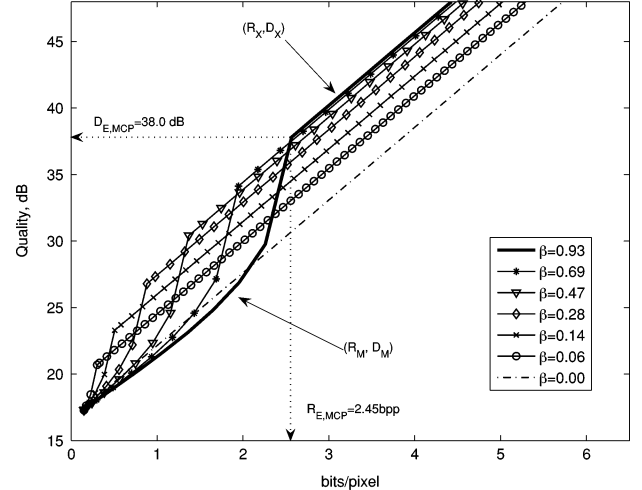Fig. 6. Rate-distortion functions for the MC-FGS with various MCP rates (β) without leaky prediction, $\sigma^2_{\Delta d} = 0.04$.

0.04 with various amounts of EL-MCP. We fixed the code rate of the BL to be $R_B = 0.1$ bits/pixel, and this rate produced a quality $D_B \triangleq 10 \log_{10}(1)/(\text{MSE}^2) = 17.3$ dB. The rate distortion performance for decoding above the MCP rate is indicated by (R_X, D_X). As can be seen from the figure, generally, a higher EL MCP rate gives a better overall compression performance if the video is decoded above the MCP rates, i.e., if there is no mismatch between the encoder and decoder predictors. However, if the decoding is below the MCP rate used for the prediction, there is a precipitous drop in performance. For example, in Fig. 6, the thick line indicates a choice of the MCP rate equal to 2.45 bpp, which produces a reference with $D_{E,\text{mcp}} = 38.0$ dB. If the amount of information received at the decoder is less than the 2.45 bpp, there is a substantial decrease in the final video quality, with performance illustrated by the rate distortion curve (R_M, D_M). This is because, at the encoder, the information up to the MCP rate is used as the reference for the prediction of the next frame, while at the decoder, a lower fidelity reference frame (below the MCP rate) is used. The portion of the curves denoted by (R_X, D_X) corresponds to the extra information (EL-Extra), which is only used for enhancing the video quality, without being used for motion compensation.

Fig. 7 illustrates the construction of the MDs using the FEC-MD approach for an OFDM system with a diversity order $N = 4$. In particular, we show the optimal parity protection levels for both the EL-MCP and the EL-Extra for various β. Recall $R_{el,\max} = 128$ descriptions $\times$ 64 RS symbols/description $\times$ 8 bits/RS symbol. In general, since the relative importance of an embedded bitstream is strictly decreasing, this results in tilted boundaries across the subcarriers, as shown in the figure, which corresponds to decreasing levels of parity protection for the codewords on the right. The vertical lines extending downward from the top show the boundaries between the EL-MCP information symbols and EL-Extra information symbols, for three values of β. By comparing the boundaries for various β, one can notice the effects of the inclusion of a partial MCP loop in the EL. In particular, the boundaries show that EL-MCP is more strongly
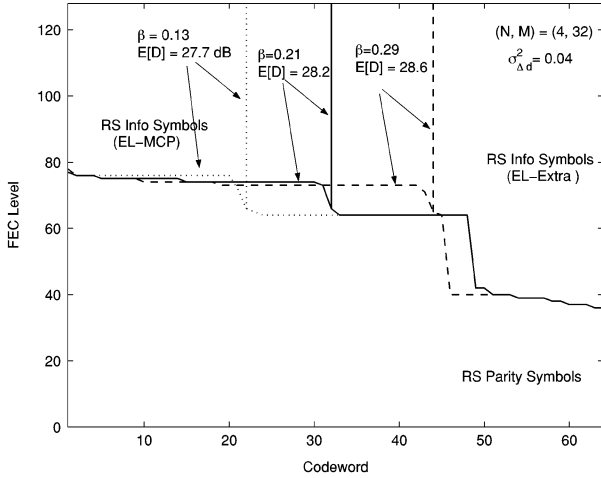
Fig. 7. RS symbol boundaries for the n-channel symmetric motion-compensated MD codes for $(N, M) = (4, 32)$ for $\sigma^2_{\Delta_d} = 0.04$.

Fig. 8. RS symbol boundaries for the n-channel symmetric motion-compensated MD codes for different numbers of independent channels N.

protected than EL-Extra, due to the drift problem associated with the loss of this information.

The boundaries separating the information symbols and parity symbols exhibit a stepwise behavior. This is mainly due to the completely correlated fading nature of the subcarriers within a subband, which results in the simultaneous loss of several MDs when the correlated subcarriers are under a deep fade. We refer interested readers to [15] for more detailed discussions.

In Fig. 8, we show the boundaries for the construction of n-channel symmetric motion-compensated MD coding for various orders of diversity, or, equivalently, different numbers of independent subbands, N. In particular, we show the optimal allocation of the parity symbols and the EL information symbols for a compression scheme with β fixed at 0.17 for systems with diversity orders $N = 2, 16, 32,$ and 128. As can be observed, the boundaries show some similar features to the still image case [15]. For instance, as the order of diversity increases, the tilting of boundaries separating the parity symbols and information symbols decreases, signifying decreasing reliance on UEP. The decrease in N also leads to staircase behavior at the boundaries due to the increase in the correlation among the subcarriers. Notice that the boundaries show similar patterns as in Fig. 7. In particular, most of the EL-MCP is strongly protected against channel errors, while the last portion the EL-MCP is relatively less strongly protected, which allows occasional minor mismatch of the encoder and decoder predictors. However, Fig. 8 also illustrates the impact of the order of diversity on the construction of the multiple individual descriptions. Specifically, as N increases, the EL-MCP symbols are spread across a larger number of descriptions/subcarriers. This may be considered undesirable from a pure source coding point of view, as more descriptions have to be received to avoid encoder-decoder mismatch. However, with a higher diversity order, the uncertainty in the number of descriptions to be correctly received decreases, meaning that the variance in the number of correctly received description decreases. As a result, the EL-MCP can be carried by a larger number of subcarriers/descriptions.
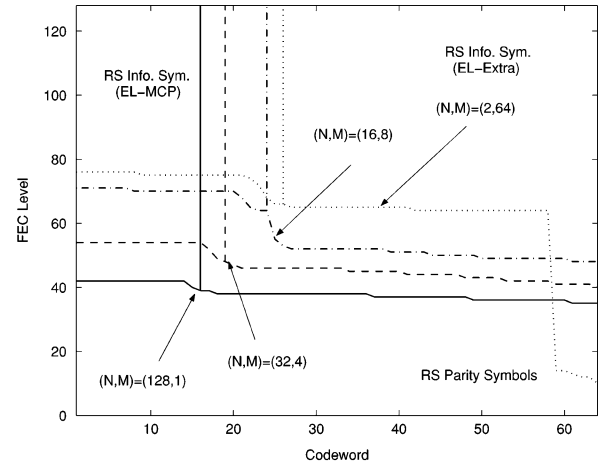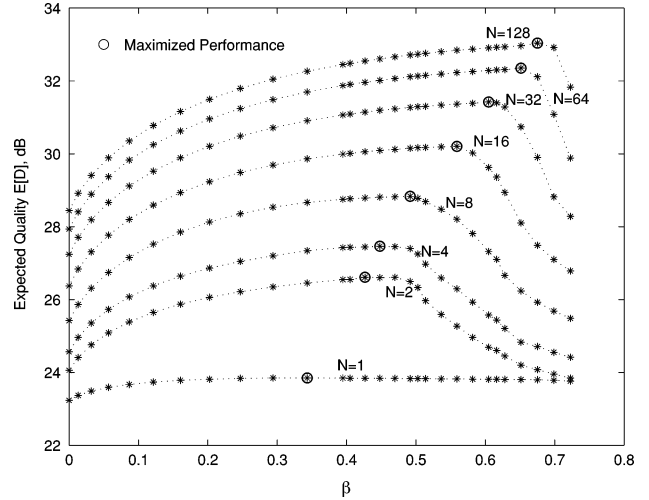

Fig. 9. Distortion performance against different β (EL-MCP) for OFDM systems with different orders of diversity N.

As stated previously, a larger MCP rate leads to higher coding efficiency at the expense of poorer error resilience. Hence, the major issue is how much information should be included for MCP so as to achieve a balanced tradeoff between the compression efficiency and error resilience. In Fig. 9, we demonstrate that knowing the diversity order can help to define the amount of EL-MCP, in terms of β and, hence, the construction of the motion-compensated MDs. We plot the distortion performance against β for systems with different diversity orders. In the plots, we also mark with a circle ($\circ$) the optimal selections of EL-MCP (β_{opt}). As can be observed, generally a better performance can be achieved with a higher diversity order. More importantly, as the diversity order N increases, β_{opt} increases and the delivered video quality improves accordingly, as shown in Fig. 10.

B. Leaky Prediction (α EL-MCP)

In this section, we study leaky prediction for controlling drift. Leaky prediction scales down the information used as the ref-
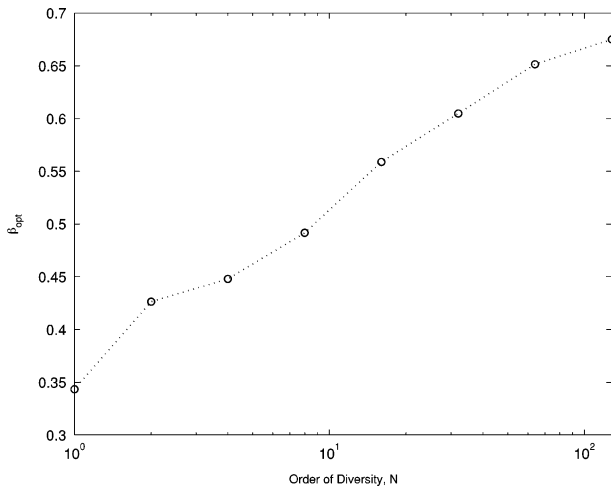
Fig. 10. Diversity order N versus β_{opt} for the proposed MD coding and transmission scheme.

Fig. 11. Rate distortion functions of MC-FGS with leaky prediction, $\sigma^2_{\Delta d} = 0.04$.

erence for MCP by a leak factor $\alpha \in [0, 1]$ so as to speed the decay of error propagation temporally. In Fig. 11, we evaluate the rate-distortion functions of two scenarios for the MC-FGS video coders with different leak factors: 1) constant bitrate and 2) constant distortion. In the figure, the solid lines represent the performance for the constant-rate scenario, in which the bitrate of the MCP is kept at 1.2 bpp, corresponding to $\beta = 0.41$, for $\alpha = 0.72$ and 1.00. As can be seen, as α increases, the quality of the reconstructed video improves if the video is decoded above the MCP rate. However, if the decoding rate is below the MCP rate, the use of a larger leak factor α also leads to a more severe drop in the final video quality, indicating poorer error resilience of the compressed video. The dashed lines in Fig. 11 represent the performance for the constant-distortion scenario, in which the quality of the reference for the EL MCP loop is fixed at $D_{E,\mathrm{MCP}} = 33.6$ dB. There are two curves, parameterized by $\alpha = 0.60$ and $\alpha = 1.00$. As can be observed, a similar tradeoff between compression efficiency and error resilience can be achieved by using different α. As shown in the figure, if the video is decoded above the MCP rate, a higher performance gain can be achieved using a larger α. However, if the video is decoded below the MCP rate, the use of a larger α leads to increasing drift, illustrated by the more substantial drop in the quality performance for $\alpha = 1.00$ in the figure.

In Fig. 12, we show the optimal boundaries for the construction of motion-compensated symmetric MDs for an OFDM system with diversity order $N = 8$. We fix the MCP rate $R_{E,\mathrm{MCP}} = 1.2$ bpp, or, equivalently $\beta = 0.46$. Hence, the results correspond to the constant-bitrate scenario. The leak factors for the MDs are $\alpha = 0.68$ and $\alpha = 0.96$. By comparing the two boundaries, one can notice the overall lower protection level of the RS parity symbols for $\alpha = 0.68$, indicating increasing error resilience of the α-attenuated motion-compensated MDs to predictor mismatch. In Fig. 13, we show the optimal boundaries for the constant-distortion scenario for $\alpha = 0.88$ and 1.00. The distortion of the EL reference is fixed at $D_{E,\mathrm{MCP}} = 28.18$ dB. Since the distortion of the reference for MCP is fixed, the bitrates, and, hence, the area marked
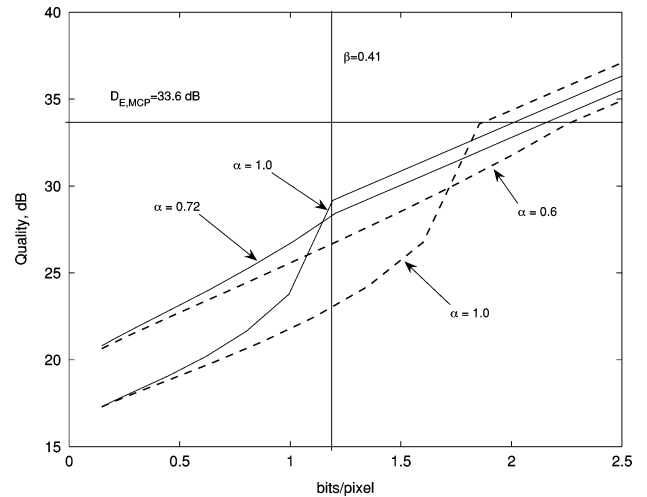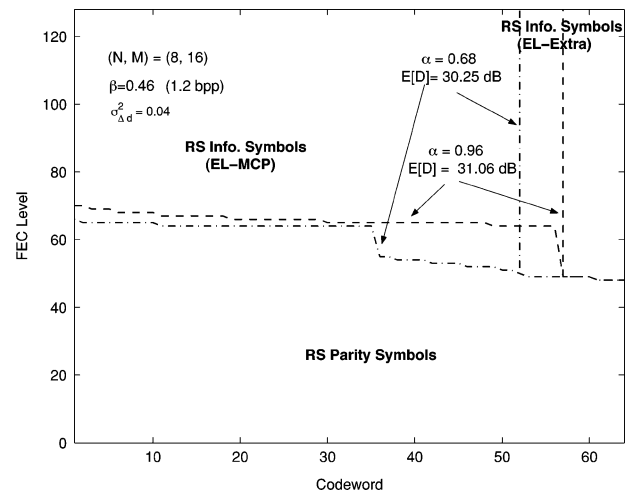

Fig. 12. RS symbol boundaries for the n-channel symmetric motion-compensated MD codes for an $(N, M) = (8, 16)$ OFDM system with EL-MCP fixed at $\beta = 0.46$ (1.2 bpp) for different α's.

EL-MCP, changes with α. Nevertheless, it can be noticed that the EL-MCP symbols are spread across a larger number of subcarriers with decreasing α, indicating an increasing error resilience of the MD codes.

Figs. 14 and 15 show the distortion performances versus α for OFDM systems with different N for the constant-bitrate and constant-distortion scenarios, respectively. Each line represents distortion performance of an OFDM system with the same order of diversity with different leaky predictors. In the plots, we mark with the symbol ($\circ$) the optimal leak factors (α_{opt}) for each curve. As can be observed, both figures show a similar feature: when the diversity order N decreases, the optimal leak factor (α_{opt}) moves to the left, corresponding to putting less weight on the EL-MCP. This is because the highly correlated nature of the subcarriers within a subband can lead to simultaneous loss of multiple MDs, creating severe predictor mismatch. The drift due to the simultaneous loss of multiple MDs as a result of the erratic behavior of the channel becomes more severe when the
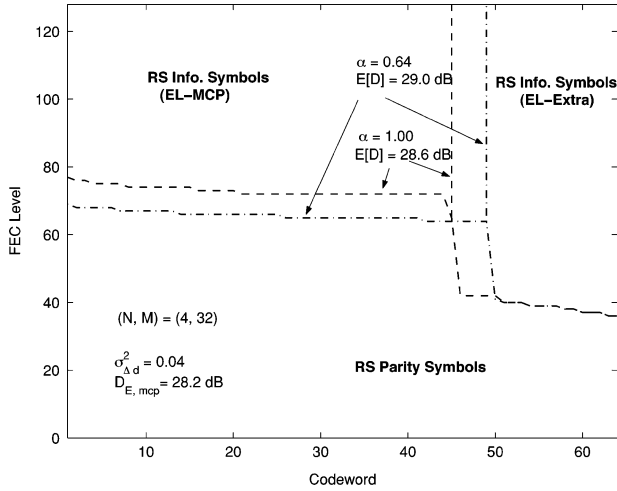
Fig. 13. RS symbol boundaries for the n-channel symmetric motion-compensated MD codes for an $(N, M) = (4, 32)$ OFDM system with quality of the reference for the EL MCP fixed at $D_{E,\mathrm{MCP}} = 28.2$ dB for different α's.
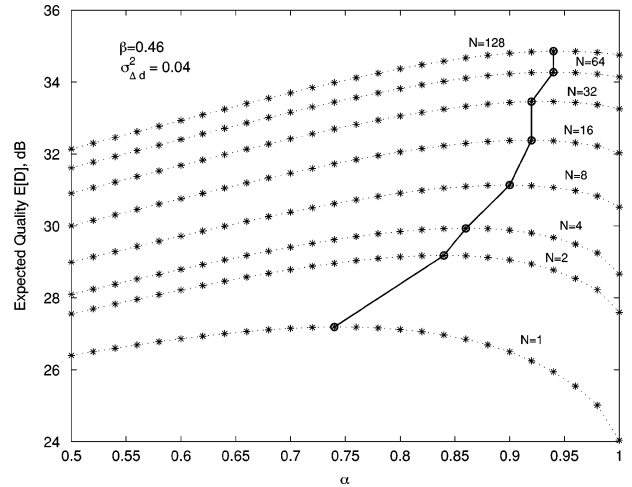

Fig. 15. Distortion performance versus α for OFDM systems with different orders of diversity N with β fixed at 0.46 corresponding to 1.2 bpp.
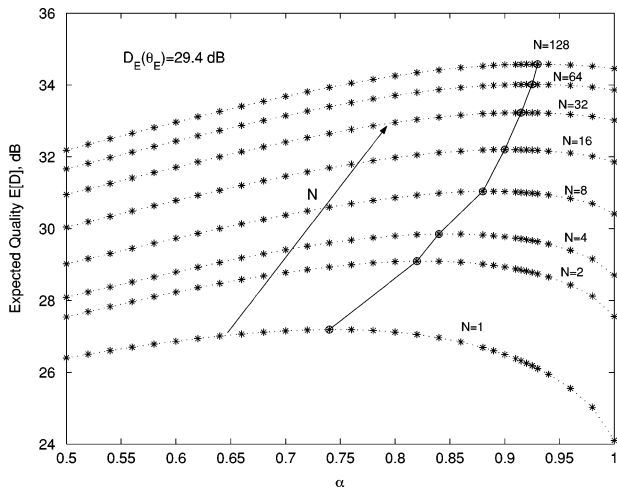

Fig. 14. Distortion performance versus α for OFDM systems with different orders of diversity N with the quality of the reference frame of the EL MCP loop fixed at $D_{E,\mathrm{MCP}} = 29.37$ dB.
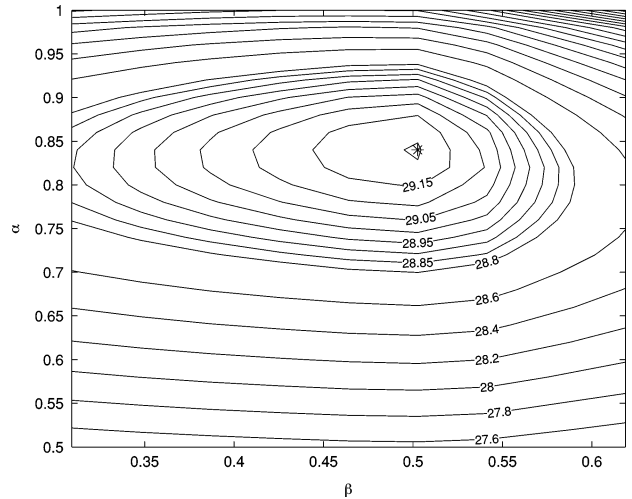

Fig. 16. Contour plot of the quality performance for different (β, α) using the n-channel symmetric motion-compensated MD codes for a system with diversity order $N = 2$.

order of diversity is small. Therefore, a smaller leak factor is preferred so as to reduce the weight of the EL-MCP.

C. Optimized Performance by Jointly Optimizing α and β

In Fig. 16, we illustrate that the performance of the n-channel symmetric motion-compensated MDs can be optimized by jointly choosing the EL-MCP, in terms of β, and the weight of the EL-MCP, in terms of α, based on the order of diversity. In particular, in Fig. 16, we show contour plots of constant distortion. That is, each contour corresponds to a constant distortion achieved by different combinations of α and β. In the figure, we indicate the optimal selection of $(\alpha, \beta)_{\mathrm{opt}}$ with the symbol $(*)$. In Fig. 17, we show a similar contour plot for an OFDM system with diversity order $N = 8$. In Fig. 17, we include the $(\alpha, \beta)_{\mathrm{opt}}$ point for systems of different diversity orders $N = 2, 8, 16$ and 32. As can be observed, as the diversity order N increases, the optimal operating point, $(\alpha, \beta)_{\mathrm{opt}}$, moves to the upper right hand part of the figure, indicating a larger α

and β can be selected due to the increasing reliability and less erratic behavior of the system.

D. Real Video Simulations

Fig. 18 shows the luminance PSNR-Y $\triangleq 10 \log_{10}(255^2/\mathrm{MSE}^2)$ versus EL bitrate for the "Foreman" sequence encoded with different EL-MCP rates. In the figure, the x-axis corresponds to the received (decoding) bit rates of the EL. As can be seen from the figure, the plots follow closely the information-theoretic prediction shown in Fig. 6. In particular, the use of a higher MCP rate can improve the overall compression efficiency, as indicated by the performance gain (measured in terms of PSNR), if the amount of the EL information received is larger than the MCP rate used in the encoder. For example, compare the curve $R_{E,\mathrm{MCP}} = 30.72$ kbps with the curve $R_{E,\mathrm{MCP}} = 10.24$ kbps. If the amount of total EL information received is, for instance, 30.72 kbps, then using $R_{E,\mathrm{MCP}} = 30.72$ kbps gives approximately 2 dB gain. However, if the amount of the EL information received is less
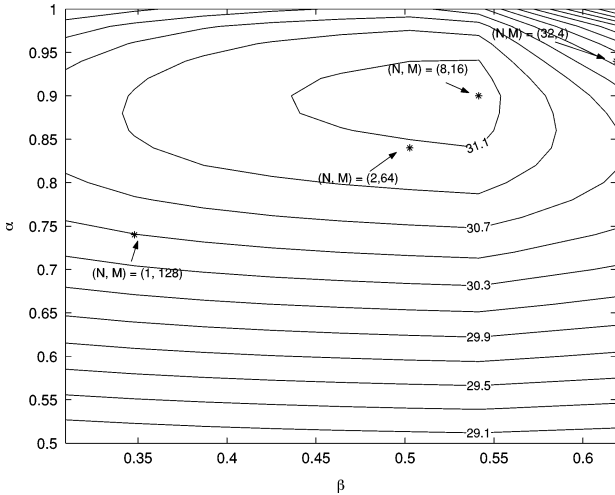
Fig. 17. Contour plot of the quality performance for different (β, α) using the n-channel symmetric motion-compensated MD codes for a system with diversity order $N = 8$ and the optimal selection of (α, β) for systems of different diversity orders N marked by $(*)$.

Fig. 19. RS symbol boundaries for the n-channel symmetric motion-compensated MD codes for different OFDM systems using the "Foreman" sequence: 1) $(N, M) = (16, 8)$, $R_{E,\text{MCP}} = 10.24$ kbps, $\alpha = 1.00$; 2) $(N, M) = (2, 64)$, $R_{E,\text{MCP}} = 15.36$ kbps, $\alpha = 0.90$.
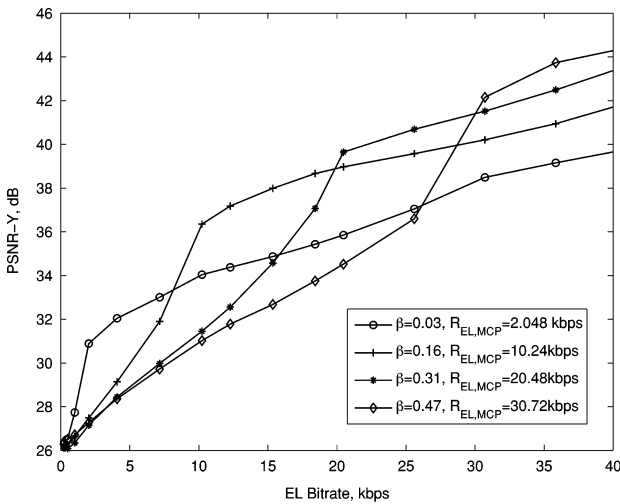

Fig. 18. PSNR-Y versus received E bitrate for the "Foreman" sequence encoded with different MCP rates, $R_{E,\text{MCP}}(\beta)$, without leaky prediction.

Fig. 20. PSNR-Y versus received EL bitrate of MC-FGS with different leaky prediction factors.

than the MCP rate, the mismatch in the predictors of the encoder and decoder can cause a substantial drop in PSNR performance, as shown in the plots. In the previous example, if the amount of the EL received is 20.48 kbps, setting $R_{E,\text{MCP}} = 10.24$ kbps instead of using $R_{E,\text{MCP}} = 30.72$ kbps gives us more than 5 dB overall improvement.

Fig. 19 shows two examples of n-channel motion-compensated MDs for the "Foreman" sequence based on the proposed scheme. The figure corresponds to the schematic plot shown in Fig. 5(b) for a total of 128 descriptions (subcarriers), in which the symbols are subdivided into EL-MCP, EL-Extra (RS information symbols) and RS parity symbols. Observe the similarity of these plots to our previous studies using the analytical video model. More importantly, the figure clearly illustrates the effects of the diversity order on the construction of motion-compensated MD codes and the necessity of stronger protection for the
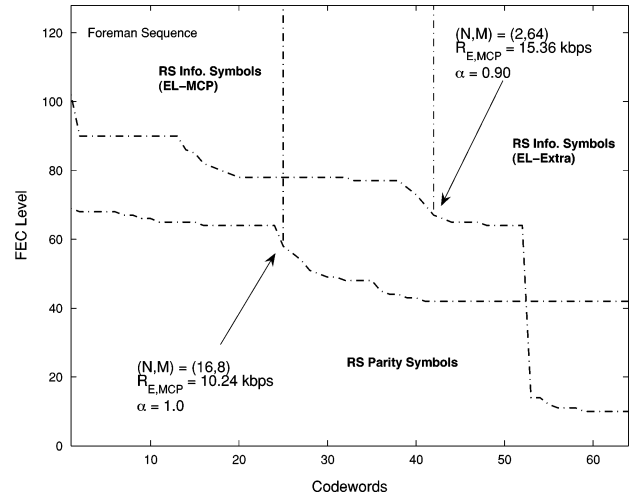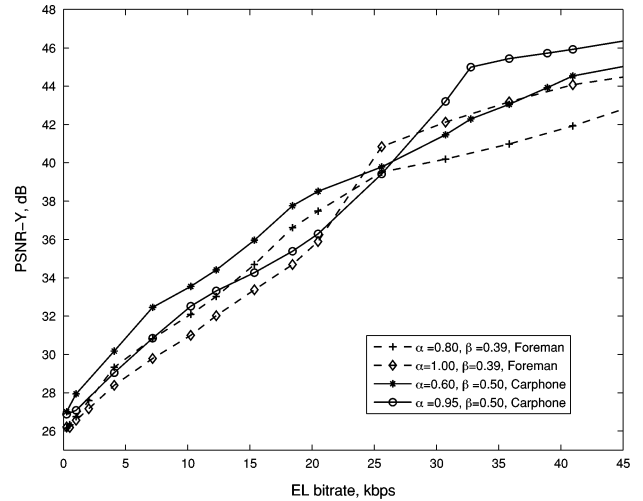
EL-MCP due to the drift problem if a portion of the EL-MCP is lost.

In Fig. 20, we show the operational rate-distortion curves of the MC-FGS codec incorporating leaky prediction. In particular, Fig. 20 shows the PSNR-Y performance against the received EL bitrate for various leak factors for both "Carphone" and "Foreman" video sequences. As can be observed from the figure, there is a substantial tradeoff using leaky prediction. In particular, as α increases, the overall compression efficiency improves if the amount of the EL information received exceeds the MCP rate, at the expense of reducing the overall error resilience, indicated by more severe performance drops.

In Fig. 21, we show the PSNR performance versus different MCP rates (α) for OFDM systems with different diversity orders using the "Foreman" sequence. In the plot, we also circle the optimized selection of the MCP rates for different OFDM systems. As can be observed, similar to our previous studies based on the analytical video model, as the diversity order of
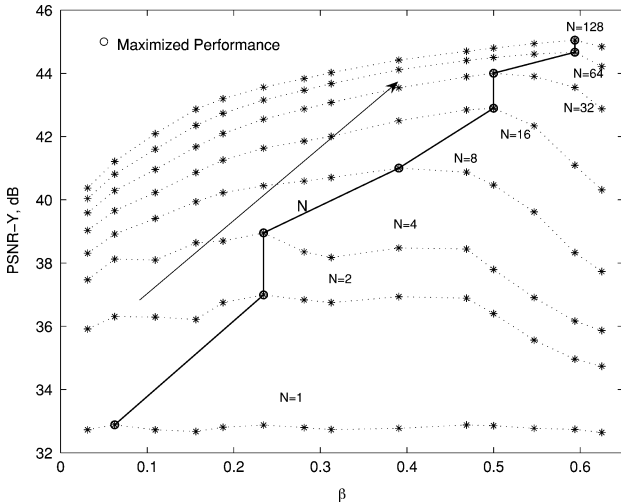
Fig. 21. PSNR-Y performance against different β (EL-MCP) using the "Foreman" sequence for OFDM systems with different diversity orders using the n-channel symmetric motion-compensated MD coding and delivery scheme.
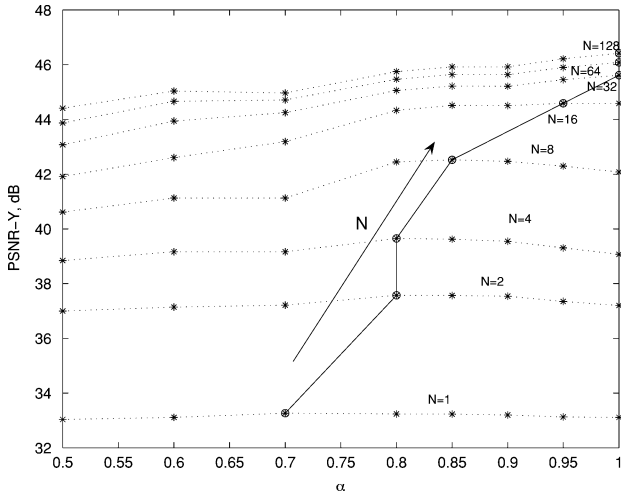

Fig. 22. PSNR-Y performance against different α (EL-MCP) using the "Carphone" sequence for OFDM systems with different diversity orders using the n-channel symmetric motion-compensated MD coding and delivery scheme.

the OFDM increases, the optimized MCP rate for the n-channel symmetric MDs could be increased to achieve a higher compression efficiency. In Fig. 21, we illustrate the PSNR performance versus different leak factors for different OFDM systems using the "Carphone" sequence. In particular, for each diversity order, we construct the MDs using different leak factors ranging from 0.5 to 1.00 in the codec. We also circle the leak factor which gives the optimal system performance. Conforming with the theoretical studies, a higher diversity order system allows one to put more weight, by using a higher α, on the information to be included in the MCP loop and to achieve a higher compression efficiency without sacrificing too much of the error-resilience property.

E. Further Discussion on the Delivery of the Base Layer (BL)

As stated previously, in this paper, we are interested in how to incorporate information on the diversity order of a communi-
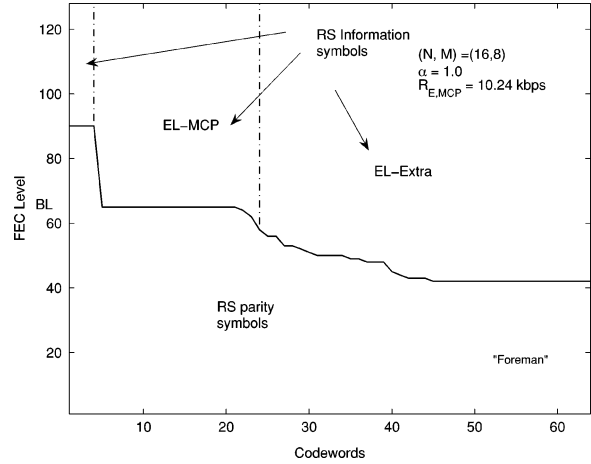

Fig. 23. RS symbol boundaries for the n-channel symmetric motion-compensated MD codes, including the BL, for different OFDM systems using the "Foreman" sequence: $(N, M) = (16, 8)$, $R_{E,\text{MCP}} = 10.24$ kbps, $\alpha = 1.00$.

cations system into the construction of n-channel motion-compensated MD codes. Hence, for simplicity, we assume reliable delivery of the BL. Since the BL carries the most important information, such as the coding modes and motion vectors, the loss of the BL could result in a catastrophic degradation in the system performance [11]. For example, in [11], it was found that the QCIF "Foreman" sequence experienced a substantial 6 dB loss in PSNR performance when the BL had a 5% packet loss rate. Our proposed approach can be easily extended to include lossy transmission of the BL. In Fig. 23, we show the construction of the n-channel symmetric MDs, including the nonscalable BL and the FGS EL (with EL-MCP and EL-Extra). In the simulation, we assume the loss of any bits in the BL would lead to decoding failure at the receiver and render the whole frame indecodable. Whenever this occurs, the lost frame is assumed to be reconstructed at its mean pixel value. As can be observed from the figure, due to the importance of the BL, the FEC protection of the BL is even stronger than that of the EL-MCP.

VI. CONCLUSION

In this paper, we studied the delivery of MC-FGS video employing an OFDM signal format on the physical layer to transmit over a frequency-selective, slow Rayleigh fading channel. We proposed an n-channel symmetric motion-compensated multiple description coding and transmission scheme, incorporating the concepts of partial and leaky predictions for mismatch control. We constructed the symmetric MDs employing a cross-layer diversity paradigm, in which we explicitly considered the diversity order of the OFDM system. We investigated the use of partial prediction, in terms of β, together with unequal error protection, to reduce the mismatch problem associated with the construction of motion-compensated MDs. We showed that knowing the diversity order can assist an MC-FGS video coder in choosing the motion-compensation prediction rate. We also investigated the use of leaky prediction, in terms of α, to achieve a tradeoff of compression efficiency and error resilience for motion-compensated MD codes. We studied two scenarios: constant-bitrate, in which the bitrate of the EL MCP is kept constant; and constant-distortion, in

which the distortion of the EL MCP reference is kept constant. Finally, we showed that the problem of drift management can be reduced, and better system performance can be achieved, by jointly optimizing β, α and the FEC protection level, and by incorporating the information on diversity order into the coding and delivery scheme using motion-compensated MD codes.

REFERENCES

[1] A. J. Goldsmith and S. B. Wicker, "Design challenges for energy-constrained Ad Hoc wireless networks," *IEEE Wireless Commun.*, vol. 9, no. 4, pp. 8–27, Aug. 2002.

[2] Y. Shen, P. C. Cosman, and L. B. Milstein, "Video coding with fixed length packetization for a tandem channel," *IEEE Trans. Image Process.*, vol. 15, no. 2, pp. 273–288, Feb. 2006.

[3] V. K. Goyal, "Multiple description coding: Compression meets the network," *IEEE Signal Process. Mag.*, vol. 18, no. 5, pp. 74–93, Sep. 2001.

[4] S. S. Pradhan, R. Puri, and K. Ramchandran, "n-channel symmetric multiple descriptions—Part I: (n, k) source channel erasure codes," *IEEE Trans. Inf. Theory*, vol. 50, no. 1, pp. 47–61, Jan. 2004.

[5] R. Puri, S. S. Pradhan, and K. Ramchandran, "n-channel symmetric multiple descriptions—Part II: (n, k) source channel erasure codes," *IEEE Trans. Inf. Theory*, vol. 51, no. 4, pp. 1377–1392, Apr. 2005.

[6] J. Ostergaard, J. Jensen, and R. Heusdens, "n-channel symmetric multiple-description lattice vector quantization," in *Proc. IEEE Data Compression Conf.*, Snowbird, UT, Mar. 2005, pp. 378–387.

[7] A. Albanese, J. Blomer, J. Edmonds, M. Luby, and M. Sudan, "Priority encoded transmission," *IEEE Trans. Inf. Theory*, vol. 46, no. 6, pp. 1737–1744, Nov. 1996.

[8] A. E. Mohr, E. A. Riskin, and R. E. Ladner, "Graceful degradation over packet erasure channels through forward error correction," in *Proc. IEEE Data Compression Conf.*, Snowbird, UT, Mar. 1999, pp. 92–101.

[9] R. Puri and K. Ramchandran, "Multiple description source coding using forward error correction codes," in *Proc. 33rd Asilomar Conf. Signals, Systems and Computer*, Pacific Grove, CA, Oct. 1999, pp. 342–346.

[10] L. Cheng, W. Zhang, and L. Chen, "Rate-distortion optimized unequal loss protection for FGS compressed video," *IEEE Trans. Broadcasting*, vol. 50, no. 2, pp. 126–131, Jun. 2004.

[11] M. van der Schaar and H. Radha, "Unequal packet loss resilience for fine-granular-scalability video," *IEEE Trans. Multimedia*, vol. 3, no. 4, pp. 381–394, Dec. 2001.

[12] R. Puri, K.-W. Lee, K. Ramchandran, and V. Bharghavan, "An integrated source transcoding and congestion control paradigm for video streaming in the Internet," *IEEE Trans. Multimedia*, vol. 3, no. 1, pp. 18–32, Mar. 2001.

[13] D. G. Sachs, R. Anand, and K. Ramchandran, "Wireless image transmission using multiple-description based concatenated codes," *Proc. SPIE*, vol. 3974, pp. 300–311, Jan. 2000.

[14] Y. Sun, Z. Xiong, and X. Wang, "Scalable image transmission over differentially space-time coded OFDM systems," in *Proc. GlobeCom*, Taipei, Taiwan, R.O.C., Nov. 2002, vol. 1, pp. 379–383.

[15] Y. S. Chan, P. C. Cosman, and L. B. Milstein, "A cross-layer diversity technique for multi-carrier OFDM multimedia networks," *IEEE Trans. Image Process.*, vol. 15, no. 4, pp. 833–847, Apr. 2006.

[16] W. Li, "Overview of fine granularity scalability in MPEG-4 video standard," *IEEE Trans. Circuits Syst. Video Technol.*, vol. 11, no. 3, pp. 301–317, Mar. 2001.

[17] A. R. Reibman, L. Bottou, and A. Basso, "Scalable video coding with managed drift," *IEEE Trans. Circuits Syst. Video Technol.*, vol. 13, no. 2, pp. 131–140, Feb. 2003.

[18] Y. Wang, A. R. Reibman, and S. Lin, "Multiple description coding for video delivery," *Proc. IEEE*, vol. 93, no. 1, pp. 57–70, Jan. 2005.

[19] M. van der Schaar and H. Radha, "Adaptive motion-compensation fine-granular-scalability (AMC-FGS) for wireless video," *IEEE Trans. Circuits Syst. Video Technol.*, vol. 12, no. 6, pp. 360–371, Jun. 2002.

[20] F. Wu, S. Li, and Y. Q. Zhang, "A framework for efficient progressive fine granularity scalable video coding," *IEEE Trans. Circuits Syst. Video Technol.*, vol. 11, no. 3, pp. 332–344, Mar. 2001.

[21] H.-C. Huang, C.-N. Wang, and T. Chiang, "A robust fine granularity scalability using trellis-based predictive leak," *IEEE Trans. Circuits Syst. Video Technol.*, vol. 12, no. 6, pp. 372–385, Jun. 2002.

[22] K. Chang and R. Donaldson, "Analysis, optimization, and sensitivity study of differential PCM systems," *IEEE Trans. Commun.*, vol. COM-20, no. 3, pp. 338–350, Jun. 1972.

[23] S. Han and B. Girod, "Robust and efficient scalable video coding with leaky prediction," in *Proc. IEEE Int. Conf. Image Processing*, Rochester, NY, Sep. 2002, vol. 2, pp. 41–44.

[24] W.-H. Peng and Y. K. Chen, "Error drifting reduction in enhanced fine granularity scalability," in *Proc. IEEE Int. Conf. Image Processing*, Rochester, NY, Sep. 2002, vol. 2, pp. 51–64.

[25] Y. Liu, Z. Li, P. Salama, and E. J. Delp, "A discussion of leaky prediction based scalable coding," in *Proc. IEEE Int. Conf. Medical Imaging*, Baltimore, MD, Jul. 2003, vol. 2, pp. 565–568.

[26] J. Apostolopoulos, W.-T. Tan, S. Wee, and G. W. Wornell, "Modeling path diversity for multiple description video communication," in *Proc. IEEE ICASSP*, Orlando, FL, May 2002, vol. 3, pp. 13–17.

[27] S. Mao, S. Lin, S. S. Panwar, Y. Wang, and E. Celebi, "Video transport over ad hoc networks: Multistream coding with multipath transport," *IEEE J. Sel. Areas Commun.*, vol. 21, no. 12, pp. 1721–1737, Dec. 2003.

[28] R. J. McEliece and W. E. Stark, "Channels with block interference," *IEEE Trans. Inf. Theory*, vol. IT-30, no. 1, pp. 44–53, Jan. 1984.

[29] M. Medard and R. G. Gallager, "Bandwidth scaling for fading multipath channels," *IEEE Trans. Inf. Theory*, vol. 48, no. 4, pp. 840–852, Apr. 2002.

[30] E. Malkamaki and H. Leib, "Performance of truncated type-II hybrid ARQ schemes with noisy feedback over block fading channels," *IEEE Trans. Commun.*, vol. 48, no. 9, pp. 1477–1487, Sep. 2000.

[31] R. Knopp and P. A. Humblet, "On coding for block fading channels," *IEEE Trans. Inf. Theory*, vol. 46, no. 1, pp. 189–205, Jan. 2000.

[32] M. Zorzi, R. R. Rao, and L. B. Milstein, "Error statistics in data transmission over fading channels," *IEEE Trans. Commun.*, vol. 46, no. 11, pp. 1468–1477, Nov. 1998.

[33] H. Bischl and E. Lutz, "Packet error rate in the non-interleaved Rayleigh channel," *IEEE Trans. Commun.*, vol. 43, no. 2/3/4, pp. 1375–1382, Feb./Mar./Apr. 1995.

[34] V. Vaishampayan, "Design of multiple description scalar quantizers," *IEEE Trans. Inf. Theory*, vol. 39, no. 3, pp. 821–834, May 1993.

[35] Y. Wang, M. T. Orchard, V. Vaishampayan, and A. R. Reibman, "Multiple description coding using pairwise correlating transforms," *IEEE Trans. Image Process.*, vol. 10, no. 3, pp. 351–366, May 2001.

[36] J. K. Rogers and P. C. Cosman, "Wavelet zerotree image compression with packetization," *IEEE Signal Process. Lett.*, vol. 5, no. 5, pp. 105–107, May 1998.

[37] X. Yang and K. Ramchandran, "Optimal subband filter banks for multiple description coding," *IEEE Trans. Inf. Theory*, vol. 46, no. 7, pp. 2477–2490, Nov. 2000.

[38] Y. Liu, P. Salama, G. W. Cook, and E. J. Delp, "Rate distortion analysis of layered video coding by leaky prediction," in *Proc. SPIE Visual Commun. Image Processing Conf.*, San Jose, CA, Jan. 2004, vol. 5308, pp. 543–554.

[39] B. Girod, "The efficiency of motion-compensating prediction for hybrid coding of video sequences," *IEEE J. Sel. Areas Commun.*, vol. 5, no. 7, pp. 1140–1154, Aug. 1987.

[40] Y. Wang and S. Lin, "Error-resilient video coding using multiple description motion compensation," *IEEE Trans. Circuits Syst. Video Technol.*, vol. 12, no. 6, pp. 438–452, Jun. 2002.

[41] A. R. Reibman, H. Jafarkhani, Y. Wang, M. T. Orchard, and R. Puri, "Multiple-description video coding using motion-compensated temporal prediction," *IEEE Trans. Circuits Syst. Video Technol.*, vol. 12, no. 3, pp. 193–204, Mar. 2002.

[42] C.-S. Kim and S.-U. Lee, "Multiple description coding of motion fields for robust video transmission," *IEEE Trans. Circuits Syst. Video Technol.*, vol. 11, no. 9, pp. 999–1010, Sep. 2001.

[43] V. Vaishampayan and S. John, "Interframe balanced multiple description video compression," in *Proc. Packet Video Workshop*, New York, Apr. 1999.

[44] V. Vaishampayan and S. John, "Balanced interframe multiple description video compression," in *Proc. IEEE Int. Conf. Image Processing*, Kobe, Japan, Apr. 1999, pp. 812–816.

[45] H. Yang, R. Zhang, and K. Rose, "Optimal end-to-end distortion estimation for drift management in scalable video coding," in *Proc. Packet Video Workshop*, Pittsburgh, PA, Apr. 2002.

[46] C. Mayer, H. Crysandt, and J. R. Ohm, "Bit plane quantization for scalable video coding," in *Proc. SPIE Visual Commun. Image Processing Conf.*, San Jose, CA, Jan. 2002, vol. 4671, pp. 1142–1152.

[47] T. Stockhammer and C. Buchner, "Progressive texture video streaming for lossy packet network," presented at the 11th Packet Video Workshop, Kyongju, Korea, May 2001.

[48] S. Dumitrescu, X. Wu, and Z. Wang, "Globally optimal uneven error-protected packetization of scalable code streams," *IEEE Trans. Multimedia*, vol. 6, no. 2, pp. 230–239, Apr. 2004.

[49] V. M. Stankovic, R. Hamzaoui, and Z. Xiong, "Real-time error protection of embedded codes for packet erasure and fading channels," *IEEE Trans. Circuits Syst. Video Technol.*, vol. 14, no. 8, pp. 1064–1072, Aug. 2004.

[50] Y. R. Zheng and C. Xiao, "Simulation models with correct statistical properties for Rayleigh fading channels," *IEEE Trans. Commun.*, vol. 51, no. 6, pp. 920–928, Jun. 2003.

[51] B. Girod, "Efficiency analysis of multihypothesis motion-compensated prediction for video coding," *IEEE Trans. Image Process.*, vol. 9, no. 2, pp. 173–183, Feb. 2000.

[52] G. J. Sullivan and R. L. Baker, "Rate-distortion optimized motion compensation for video compression using fixed and variable size blocks," in *Proc. IEEE GlobeCom*, Phoenix, AZ, Nov. 1991, pp. 85–90.

[53] M. Flierl and B. Girod, *Video Coding with Superimposed Motion-Compensated Signals: Application to H.264 and Beyond*. Boston, MA: Kluwer, 2004.

[54] T. Berger, *Rate Distortion Theory: A Mathematical Basis for Data Compression*. Englewood Cliffs, NJ: Prentice-Hall, 1971.

[55] G. W. Cook, J. Prades-Nebot, Y. Liu, and E. J. Delp, "Rate-distortion analysis of motion compensated rate scalable video," *IEEE Trans. Image Process.*, vol. 15, no. 8, pp. 2170–2190, Aug. 2006.

Pamela C. Cosman (S'88–M'93–SM'00–F'08) received the B.S. degree (with honors) in electrical engineering from the California Institute of Technology, Pasadena, in 1987, and the M.S. and Ph.D. degrees in electrical engineering from Stanford University, Stanford, CA, in 1989 and 1993, respectively.

She was an NSF postdoctoral fellow at Stanford University and a Visiting Professor at the University of Minnesota during 1993–1995. In 1995, she joined the faculty of the Department of Electrical and Computer Engineering, University of California, San Diego, where she is currently a Professor and Director of the Center for Wireless Communications. Her research interests are in the areas of image and video compression and processing.

Dr. Cosman is the recipient of the ECE Departmental Graduate Teaching Award (1996), a Career Award from the National Science Foundation (1996–1999), and a Powell Faculty Fellowship (1997–1998). She was a Guest Editor for the IEEE JOURNAL ON SELECTED AREAS IN COMMUNICATIONS June 2000 Special Issue on Error-Resilient Image and Video Eoding, and was the Technical Program Chair of the 1998 Information Theory Workshop, San Diego. She was an Associate Editor of the IEEE COMMUNICATIONS LETTERS (1998–2001), and an Associate Editor of the IEEE SIGNAL PROCESSING LETTERS (2001–2005). She was a Senior Editor (2003–2005), and is now the Editor-in-Chief, of the IEEE JOURNAL ON SELECTED AREAS IN COMMUNICATIONS. She is a member of Tau Beta Pi and Sigma Xi.

Laurence B. Milstein (S'66–M'68–SM'75–F'85) received the B.E.E. degree from the City College of New York, New York, in 1964, and the M.S. and Ph.D. degrees in electrical engineering from the Polytechnic Institute of Brooklyn, Brooklyn, NY, in 1966 and 1968, respectively.

From 1968 to 1974, he was with the Space and Communication Group of Hughes Aircraft Company, and from 1974 to 1976, he was a Member of the Department of Electrical and Systems Engineering, Rensselaer Polytechnic Institute, Troy, NY. Since 1976, he has been with the Department of Electrical and Computer Engineering, University of California at San Diego (UCSD), La Jolla, where he is a Professor and former Department Chairman, working in the area of digital communication theory, with special emphasis on spread-spectrum communication systems. He has also been a Consultant to both government and industry in the areas of radar and communications.

Dr. Milstein was an Associate Editor for communications Theory for the IEEE TRANSACTIONS ON COMMUNICATIONS, an Associate Editor for Book Reviews for the IEEE TRANSACTIONS ON INFORMATION THEORY, an Associate Technical Editor for the IEEE Communications Magazine, and the Editor-in-Chief of the IEEE JOURNAL ON SELECTED AREA IN COMMUNICATIONS. He was the Vice President for Technical Affairs in 1990 and 1991 of the IEEE Communications Society, has been a member of the Board of Governors of both the IEEE Communications Society and the IEEE Information Theory Society, and is a former Chair of the IEEE Fellows Selection Committee. He is a recipient of the 1998 Military Communications Conference Long-Term Technical Achievement Award, an Academic Senate 1999 UCSD Distinguished Teaching Award, an IEEE Third Millenium Medal in 2000, the 2000 IEEE Communication Society Armstrong Technical Achievement Award, the 2002 MILCOM Fred Ellersick Award, and the Ericsson Endowed Chair in Wireless Communication Access Techniques in 2005.

Yee Sin Chan (S'00–M'03) received the B.Eng. (Hons.) degree in electrical and electronic engineering from the University of Hong Kong (HKU), the M.Phil. degree in physics from the Hong Kong University of Science and Technology (HKUST), and the M.Sc. and Ph.D. degrees in electrical engineering from Rensselaer Polytechnic Institute, Troy, NY.

From 2003 to 2005, he was a Postdoctoral Research Scientist at the University of California at San Diego, La Jolla, CA. From 2005 to 2006, he was a Visiting Assistant Professor in the Department of Electrical and Computer Engineering, University of Miami, Coral Gables, FL. He was an Electrical Engineer at NextWave Broadband, San Diego, CA, in 2006. Since December 2006, he has been with Verizon. Currently, he is a Distinguished Member of Technical Staff at Verizon Corporate Technology, Walnut Creek, CA. His research interests lie in the areas of communications, signal processing, and information theory.

Dr. Chan has received several awards, including the Sir Edward Youde Fellowship from the Hong Kong Government, the Y. L. Liu Fellowship from RPI, and the Joyce M. Kuok Scholarship from HKU. He is a member of Sigma Xi.